Quaternary International 354 (2014) 110–121

Contents lists available at ScienceDirect

Quaternary International

journal homepage: www.elsevier.com/locate/quaint

New remains of *Rhinoceros* (Rhinocerotidae, Perissodactyla, Mammalia) associated with *Gigantopithecus blacki* from the Early Pleistocene Yanliang Cave, Fusui, South China

Yaling Yan [a,b], Yuan Wang [a,c,*], Changzhu Jin [a], Jim I. Mead [c]

[a] Key Laboratory of Vertebrate Evolution and Human Origins of Chinese Academy of Sciences, Institute of Vertebrate Paleontology and Paleoanthropology, Chinese Academy of Sciences, Beijing 100044, China
[b] University of Chinese Academy of Sciences, Beijing 100049, China
[c] Department of Geosciences, Don Sundquist Center of Excellence in Paleontology, East Tennessee State University, Johnson City, TN 37614, USA

ARTICLE INFO

Article history:
Available online 23 January 2014

ABSTRACT

Abundant dental fossils of *Rhinoceros*, associated with *Gigantopithecus blacki* from the early Early Pleistocene Yanliang Cave deposits in Fusui County, Guangxi Zhuang Autonomous Region of southern China, are described as *Rhinoceros fusuiensis* sp. nov. (Rhinocerotidae, Perissodactyla, Mammalia). The new species is morphologically more similar to the extant species *Rhinoceros sondaicus* (Javan rhinoceros) than to other species of the genus, but differs from *R. sondaicus* in bearing a slightly smaller size, a complete protoloph on P2 after heavily worn, a better developed crochet which is close to the protoloph, and a more curved ectoloph. *Rhinoceros fusuiensis* sp. nov. is considered as the potential ancestor of the living *R. sondaicus* and the common element of the Early Pleistocene *Gigantopithecus-Sinomastodon* fauna in southern China. The *Rhinoceros* remains from other Early Pleistocene sites (e.g., Longgupo Cave and Mohui Cave in southern China and Irrawaddy sediments in Myanmar) are also assigned into the new species. The discovery of *R. fusuiensis* sp. nov. provides important information on Quaternary biostratigraphy in southern China, as well as implicating southern China as a significant evolutionary and zoogeographic center for *Rhinoceros* during the Early Pleistocene.

1. Introduction

Extant Rhinoceroses (Rhinocerotidae, Perissodactyla) are currently composed of four genera and five species (Nowak, 1999): *Diceros bicornis* and *Ceratotherium simum* in Africa and *Rhinoceros unicornis*, *Rhinoceros sondaicus*, and *Dicerorhinus sumatrensis* in South and Southeast Asia. In the fossil record, however, the family was widely distributed throughout much of Eurasia, North America, and Africa. During the Quaternary there were two fossil species of *Rhinoceros* recognized in China including *Rhinoceros sinensis* and *R. sondaicus* (Wu, 1983; Tong and Moigne, 2000), and most of the *Rhinoceros* remains are attributed to *R. sinensis* (Tong, 2001).

Rhinoceros sinensis was erected by Owen (1870) based on a few isolated fossil teeth without locality and horizon details, except they were supposedly from Chongqing in southern China. Subsequently, Colbert and Hooijer (1953) discussed the systematics of *R. sinensis* when they studied the Middle Pleistocene Yanjinggou (=Yenchingkou) fauna from Chongqing (formerly Sichuan) in southern China, where abundant *Rhinoceros* remains have been found during the past twenty years (Tong, 2001). Nevertheless, the taxonomy of Pleistocene *Rhinoceros* in southern China is still confused and ill-defined because of the common practice to identify rhinocerotid remains using the "waste-basket" taxon, *R. sinensis*, without detailed description and well-defined characteristics (Tong and Moigne, 2000; Tong, 2001; Chen et al., 2012).

Recently, a great variety of *Gigantopithecus blacki* and *Homo sapiens* remains (Zhao et al., 2008; Jin et al., 2009a, b, 2014; Liu et al., 2010; Zhang et al., 2014) have been recovered in association with other abundant vertebrate fossils (Jin et al., 2008, 2010; Wang et al., 2009, 2010, 2014; Zhang et al., 2010; Dong et al., 2011, 2013, 2014; Harrison et al., 2014; Mead et al., this volume) from the Quaternary karst caves of Zuojiang River area, Guangxi Zhuang Autonomous Region (ZAR), South China. Especially, a large number of *Rhinoceros* dental remains have been found from the Early Pleistocene Yanliang Cave, Fusui County. The present study aims to

* Corresponding author. Key Laboratory of Vertebrate Evolution and Human Origins of Chinese Academy of Sciences, Institute of Vertebrate Paleontology and Paleoanthropology, Chinese Academy of Sciences, 142 Xizhimenwai Street, Beijing 100044, China.
E-mail address: xiaowangyuan@ivpp.ac.cn (Y. Wang).

1040-6182/$ – see front matter © 2014 Elsevier Ltd and INQUA. All rights reserved.
http://dx.doi.org/10.1016/j.quaint.2014.01.004

provide a detailed morphological study of these valuable *Rhinoceros* materials, as well as their implications for Quaternary biostratigraphy in southern China.

2. Geological and faunal setting

Yanliang Cave (22°13′54″N, 107°36′35″E) is about 16 km southeast of the Chongzuo Ecological Park and is located on the Gaoyan Mountain, Fusui County, Chongzuo City, Guangxi ZAR (Fig. 1). Fusui is located in a bare karst area and has a moist monsoon climate typical of the northern tropics. On the steep faces of the karst slopes, numerous caves of various dimensions have been formed, most of which contain fossiliferous deposits. As a consequence of the continuous uplift of this area since the Quaternary, multiple horizons of karst caves with different elevations have been developed. Generally, the higher the elevation of a cave, the older its age (Jin et al., 2009a, b, 2014).

The natural entrance of Yanliang Cave is south-facing. The cave is about 18 m long, with a maximum width of 10 m. The elevation of the floor of the cave entrance is about 200 m above sea level, which lies in the fifth horizon of the Chongzuo karst cave system and corresponds to *Gigantopithecus*-bearing Early Pleistocene sediments (Jin et al., 2009a, b). The cave sediments are composed of grayish white calcareous speleothems, yellow sands, yellowish brown silts with numerous tiny breccias and red clays. The stratigraphic sequence can be divided into 4 levels from top to bottom with a total thickness of approximately 6.8 m. Most mammalian fossils including *G. blacki* and *Rhinoceros* were recovered from the third level (Fig. 2).

After the excavation, at least 40 large and small mammalian species were recovered, including *G. blacki*, *Pachycrocuta licenti*, *Tapirus sanyuanensis*, *Hesperotherium sinensis*, *Typhlomys intermedius*, *Chiropodomys primitivus*, *Niviventer preconfucianus*, and *Leopoldamys edwardsioides* (Fig. 3), which are the typical elements of the Early Pleistocene "*Gigantopithecus* fauna" (Jin et al., 2008, 2009a, 2014) or "*Gigantopithecus-Sinomastodon* fauna" (Wang et al., 2014) in southern China. Based on the faunal analysis, the geological age of Yanliang fauna is estimated to be the early Early Pleistocene, which is roughly contemporaneous with Baikong fauna (2.0 Ma) in the same area (Jin et al., 2014), as well as with Longgupo, Liucheng, Mohui and Chuifeng faunas (Han, 1987; Pei, 1987; Huang and Fang, 1991; Wang, 2005, 2009; Wang et al., 2005, 2007).

3. Materials and methods

The *Rhinoceros* specimens described herein are archived in the collection of the Institute of Vertebrate Paleontology and Paleoanthropology (IVPP), Chinese Academy of Science, Beijing, China. Measurements (mm) are made with a digital caliper for teeth. Taxonomy used in this paper follows Prothero and Schoch (1989a). The dental terminology is modified from Guérin (1980) and Qiu and Wang (2007) (Fig. 4). The institutional abbreviations are as follows.

AMNH: American Museum of Natural History, New York, USA
CV: Chongqing Natural Museum, Chongqing, China
IVPP (V): Institute of Vertebrate Paleontology and Paleoanthropology, Chinese Academy of Sciences, Beijing, China
NMMP-KU-IR: National Museum of Myanmar Paleontology-Kyoto University-Irrawaddy

4. Systematic paleontology

Class Mammalia Linnaeus, 1758
Order Perissodactyla Owen, 1848
Family Rhinocerotidae Owen, 1845
Subfamily Rhinocerotinae Owen, 1845
Genus *Rhinoceros* Linnaeus, 1758

Type species. *R. unicornis* Linnaeus, 1758
Other included species. *R. sondaicus* Desmarest, 1822; *Rhinoceros sivalensis* Falconer and Cautley, 1847; *R. sinensis* Owen, 1870; *Rhinoceros fusuiensis* sp. nov.
Stratigraphic range. Late Miocene to present.

R. fusuiensis sp. nov.
Synonyms
1991. *Rhinoceros* cf. *sinensis* (Owen) – Huang and Fang, p.120, pl.4
2005. *R. sinensis* (Owen) – Wang W, pp.87–88, pl.13
2006. *R. sondaicus* (Desmarest) – Zin-Maung-Maung-Thein et al., pp.198, fig.3

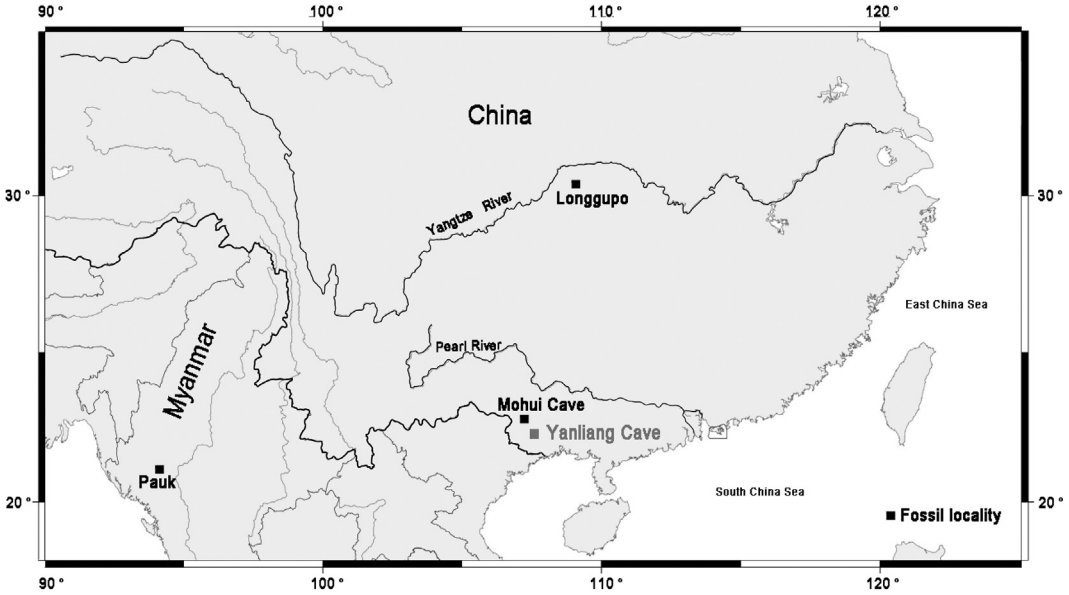

Fig. 1. Map showing the fossil localities of *Rhinoceros fusuiensis* sp. nov.

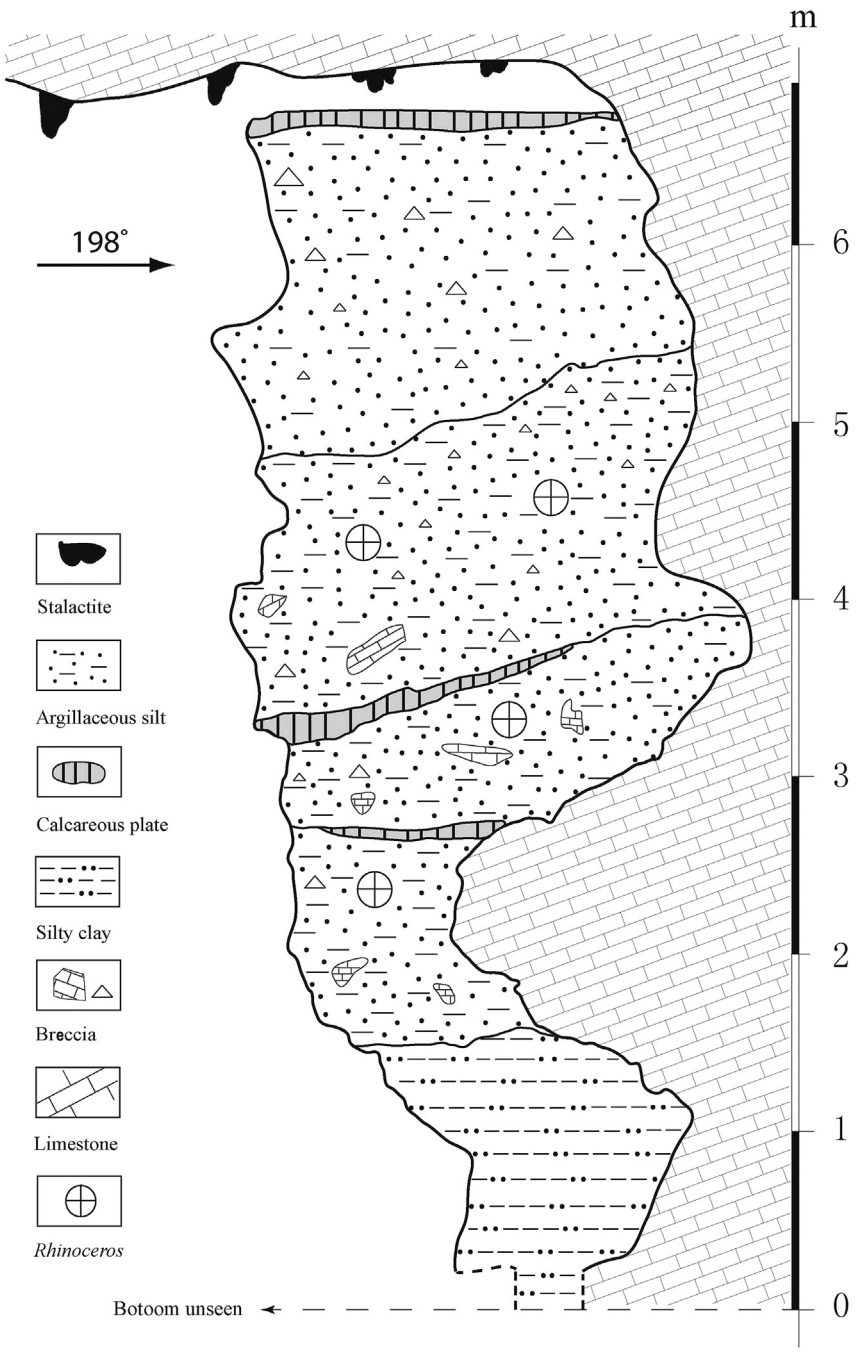

Fig. 2. The stratigraphic sequence of Yanliang Cave.

4.1. Holotype

One complete left M3 (IVPP V18642.47).

4.2. Referred materials

Four DP1s (V18642.1–4), four DP2s (V18642.5–8), three DP3s (V18642.9–11), twelve P2s (V18642.13–24), five P3s (V18642.25–29), six P4s (V18642.30–35), six M1s (V18642.12, 36–40), six M2s (V18642.41–46), seven M3s (V18642.48–54), seven upper incisors (I1s, V18642.55–61); one dp2 (V18642.62), six dp3s (V18642.63–68), five dp4s (V18642.69–73), eighteen p2s (V18642.74–91), nine p3s (V18642.74–91), twelve p4s (V18642.74–91), thirteen m1s (V18642.113–125), nine m2s (V18642.126–134), five m3s (V18642.135–139), seven lower incisors (i2s, V18642.142–146,159, 160).

4.3. Type locality and age

Yanliang Cave, Fusui County, Chongzuo City, Guangxi ZAR, South China; the early Early Pleistocene (~2.0 Ma).

4.4. Etymology

Specific name is derived from Chinese “Fusui”, the name of the fossil locality.

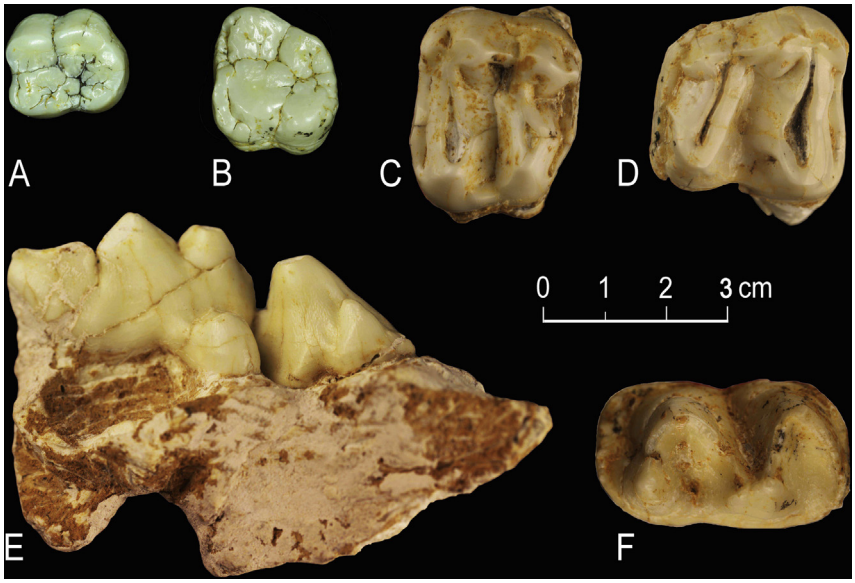

Fig. 3. The typical mammalian specimens collected from Yanliang Cave. A–B, *Gigantopithecus blacki* (CFLGYL 806, CFLGYL 803), right m1/2 (A) and left M3 (B); C–D, *Tapirus sanyuanensis* (CFLGYL 910, 911), left P4 (C) and right M2 (D); E, *Pachycrocuta licenti* (CFLGYL 825), a right maxilla with P3–P4; F, *Hesperotherium sinensis* (CFLGYL 901), left m3. A–D and F, occlusal view; E, lingual view. CFLGYL, the number of field.

4.5. Diagnosis

Relatively smaller dental size with subhypsodont crown. The I1 and DP1 are present while the i2 is robust. The paracone rib and metacone rib are weak on P2, while prominent on P3 and P4. On M1–M3, the paracone rib is present and the metacone rib is degenerated or missing. The cristae are only observed on the upper deciduous dentition, not on the upper permanent dentition. The crochets are moderately to strongly developed. The well-developed crochet has no link to the protoloph, so the medifossette is absent. The crochet and ectoloph form a sharp angle. The antecrochet is absent. Both parastyle and metastyle are present. The protocone constriction is weak. On P2, the hypocone extends to the median valley so it is wider than the protocone. On P3–M2, the metaloph is narrower than the protoloph. Both of the anterior and posterior cingula are developed on the upper dentition. The entrance to the median valley is broad, and the depth of postfossette is equivalent to or shallower than that of the median valley on the upper dentition. The protoloph on P2 can be observed after heavy wear. On M1 and M2, the ectoloph is concave in the posterior part and is inclined to the lingual side. The crown of M3, without metacone rib, is triangular in occlusal outline. The length of the ectometaloph is

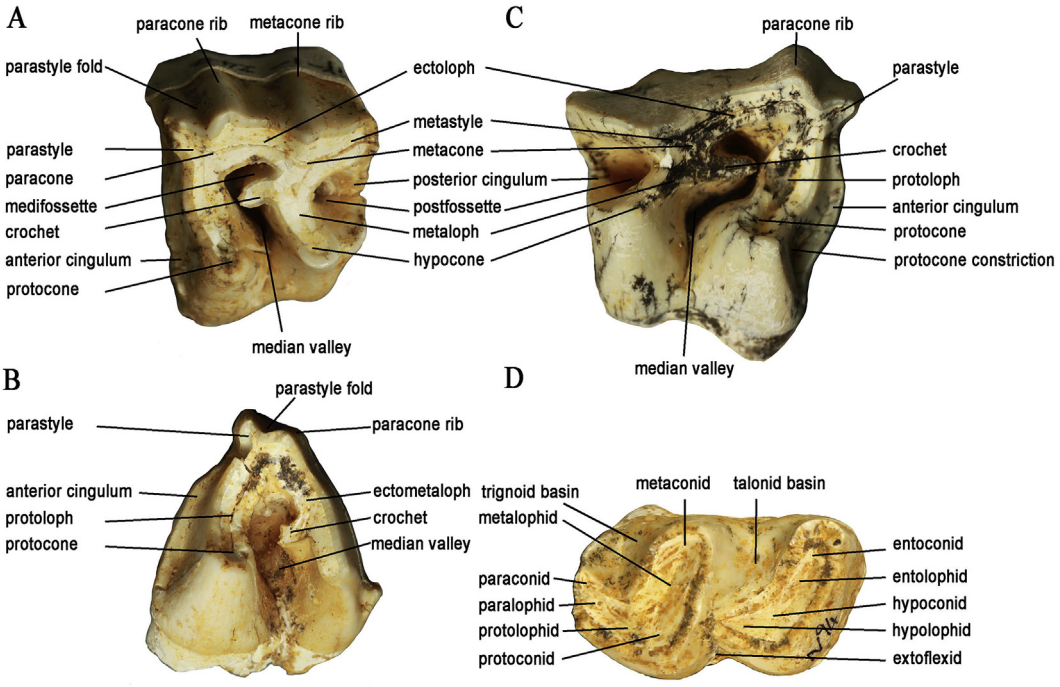

Fig. 4. The schematic representation of cheek teeth occlusal morphology of *Rhinoceros*. A, left P3 (V18462.25); B, left M3 (V18462.48); C, right M1 (V18462.40); D, left m2 (V18462.129).

longer than its height on the unworn M3. The crown of the unworn premolar is higher than that of the molar.

4.6. Measurements

All measurements are presented in Tables 1 and 2.

Table 1
Measurements of the upper teeth of different species of *Rhinoceros* and *Dicerorhinus* (in mm).

		R. fusuiensis sp. nov.	*R. sinensis*		*D. sumatrensis*[c]	*R. unicornis*[c]	*R. sondaicus*[c]
		Yanliang Cave	Yanjinggou[a]	Longgudong[b]			
P2	*N*	9	5	11			
	L	27.7–36.3 (31.4)	26–33 (29.4)	25.5–34 (30.5)	27–32 (29.6)	37–45.5 (40.9)	30–38.5 (34.7)
	W_a	27.5–38.7 (32.0)	36–45 (41.4)	30.0–43.4 (35.7)	27–36.5 (32.1)	43–48 (45.7)	34.5–44 (39.8)
	W_p	30.8–38.8 (33.5)	41–50 (45.0)	32.5–45.5 (37.7)			
P3	*N*	4	8	8			
	L	34.2–38.8 (36.0)	32–42 (36.8)	31.3–37.8 (35.3)	33.5–37.5 (35.6)	43–50 (47.8)	36.5–50 (41.3)
	W_a	43.9–50 (46.3)	51–63 (56.1)	46–55.5 (49.8)	37–47 (40.7)	55.5–60.5 (58.3)	42–55 (49.6)
	W_p	38.3–50.5 (42.9)	49–58 (52.4)	43–54 (47.1)			
P4	*N*	7	10	7			
	L	34.8–43.9 (39.6)	35–48 (39.6)	34–47 (40.7)	36–39 (37.3)	42–51 (46)	41–47.5 (43.8)
	W_a	45.3–53.8 (50.1)	57–70 (62.2)	49.9–60 (54.6)	42.5–51.5 (46.1)	59–69.5 (64)	52–59 (54.9)
	W_p	40.7–48.4 (44.6)	52–61 (56.8)	46–54.5 (50.8)			
M1	*N*	4	9	7			
	L	47–50.6 (48.5)	41–55 (47.4)	45.8–54.3 (49.3)	46–51.5 (47.9)	48–58 (53.3)	46–51 (48.9)
	W_a	48.2–56.0 (51.4)	63–81 (68.7)	53–69.5 (58.4)	46.5–54 (49.4)	62–72.5 (65.7)	52.5–60 (55.8)
	W_p	35.1–42.0 (37.2)	58–76 (63.8)	49.5–60.7 (54.4)			
M2	*N*	5	10	10			
	L	47.7–53.5 (49.7)	45–60 (57.8)	46.8–57.8 (51.4)	47.5–55 (50.4)	53–62 (57.6)	44.5–55 (50.5)
	W_a	52.5–58.3 (55.1)	63–82 (72.4)	53.0–65.5 (58.4)	48–57 (51.8)	64.5–76 (68.6)	53–62.5 (57.5)
	W_p	37.4–49.9 (43.1)	56–75 (63.6)	47.5–56 (48.6)			
M3	*N*	7	5	7			
	Los	44.0–55.2 (50.8)	46–56 (51.6)	42.7–52.5 (47.2)	47.5–56 (50.8)	59–65 (63)	44.5–61.5 (51.8)
	W	44.2–50.6 (48.9)	57–71 (62.8)	49–59 (53.5)	44.5–47.5 (46.2)	56–68.5 (61.9)	43.5–57 (50.4)

[a] Colbert and Hooijer, 1953.
[b] Zheng, 2004.
[c] Guérin, 1980.

Table 2
Measurements of the lower teeth of different species of *Rhinoceros* and *Dicerorhinus* (in mm).

		R. fusuiensis sp. nov.	*R. sinensis*		*D. sumatrensis*[c]	*R. unicornis*[c]	*R. sondaicus*[c]
		Yanliang Cave	Yanjinggou[a]	Longgudong[b]			
p2	*N*	15	4	7			
	L	22.6–29.4 (25.4)	30–34 (31.8)	27.5–35 (32.2)	24–27 (25)	31–32 (31.3)	25–29.5 (27.7)
	W	14.5–19.8 (17.1)	15–22 (19.3)	20.5–24.3 (22.1)	14–16.5 (15.1)	21.5–24.5 (22.9)	21–21 (17.9)
p3	*N*	7	3	5			
	L	29.7–36.4 (33.8)	39	34.8–42.3 (38.1)	27–33.5 (30.4)	38–42 (40.3)	33–39 (36)
	W	19.0–24.8 (22.0)	26–28 (26.7)	22.8–27.4 (24.5)	18.55 (20.4)	27–32 (29.1)	22–27.5 (24.5)
p4	*N*	12	2	13			
	L	32.3–45.0 (38.1)	45–46 (45.5)	34.8–42.3 (38.1)	32–38 (33.8)	41–46 (43.8)	36.5–42.5 (39.1)
	W	21.8–24.5 (23.4)	30	23.5–31.5 (28.3)	21.5–25 (23)	29–34 (31)	24–29 (26.9)
m1	*N*	13	7	18			
	L	40.0–46.6 (42.7)	48–55 (51.9)	36.5–52.3 (45.3)	31–40.5 (37.9)	46–48 (46.8)	41–46.5 (43.6)
	W	22.1–28.0 (24.8)	31–36 (33.1)	26–31.8 (29)	23–27.5 (25.3)	28–32.5 (30.1)	26–32 (28.8)
m2	*N*	9	6	14			
	L	37.1–48.9 (43.6)	49–61 (55.3)	43–51.5 (47.9)	39–47.5 (43.3)	52–56.5 (54.1)	40.5–51 (46.2)
	W	24.5–26.9 (25.9)	29–37 (33)	25.8–35.5 (29.1)	23.5–28 (26.1)	31–36 (32.5)	27–32.5 (29.4)
m3	*N*	3	2	3			
	L	46.5–48.3 (47.3)	51–57 (54)	48.5–51 (49.9)	43–48 (45.1)	49.5–60 (57.5)	41–53 (47.7)
	W	23.7–25.6 (24.5)	30–34 (32)	29.3–33.2 (31.3)	23.5–26 (24.8)	29–35 (30.9)	24.5–29.5 (27.2)

[a] Colbert and Hooijer, 1953.
[b] Zheng, 2004.
[c] Guérin, 1980.

4.7. Description

4.7.1. Deciduous dentition

4.7.1.1. DP1 (n = 4, Fig. 5 A, B). The crown of DP1 has simple morphology, and it is reversed trapezoidal in occlusal outline. The complete metaloph is formed after moderate wear and the isolated protocone is separated from the ectoloph. The protocone and hypocone are connected after heavily worn. A slight apophysis appears on the buccal surface of the ectoloph, and the paracone rib and metacone rib are weak. The ectoloph is almost perpendicular to the metaloph. The posterior cingulum is well developed, and the postfossette is shallower than the median valley.

4.7.1.2. DP2 (n = 4, Fig. 5 C). The crown of DP2 is trapezoidal in occlusal outline, with a wider buccal side than a lingual one. The mesocone rib is strongly developed. The distinct crochet and crista are connected to form the medifossette. The anterior and posterior cingula and the postfossette are well developed. The protocone constriction is weak or even absent.

4.7.1.3. DP3 (n = 3, Fig. 5 D). The crown of DP3 is nearly square in occlusal outline. The parastyle and metastyle are prominent. The paracone rib is distinct on the buccal surface of the ectoloph from the top to the root. There is a gap between the well-developed crochet and protoloph, exceeding the half width of the median valley. The crista is missing, and the anterior and posterior cingula are well developed. The position of the anterior cingulum becomes gradually lower from the buccal to the lingual side and the postfossette is deeper than the median valley. The base of the protoloph is inflated, of which width is about two-thirds of the lingual width of the crown. There is a broad entrance to the median valley with no tuber. The protocone constriction is weak.

4.7.1.4. dp2 (n = 1, Fig. 5 E). The crown is triangular in occlusal outline. Both the metaconid and entocoind are elongate to form a closed enamel loop on the talonid with deep wear. The ectoflexid is present.

4.7.1.5. dp3 (n = 6, Fig. 5 F). The dp3 is larger than dp2. The length is longer than width. The paralophid and protolophid extend to the lingual and anterior sides respectively, and nearly form a right angle. The outline of the trigonid is almost rectangular. The talonid basin is deeper than the trigonid basin.

4.7.1.6. dp4 (n = 5, Fig. 5 G). With the largest size among all the deciduous teeth, dp4 is similar to dp3 in dental morphology. The main cusps on the lingual side (paraconid, metaconid and entoconid) are higher than those on the buccal side (protoconid and hypoconid). The paralophid is small on worn specimens. The trigonid basin is slightly shallower than the talonid basin.

4.7.2. Permanent dentition

4.7.2.1. P2 (n = 12, Fig. 6 A–D). The length is shorter than the width. Paracone rib and metacone ribs are weak on the buccal surface of the ectoloph. The parastyle and metastyle are prominent and the protocone constriction is absent. The crochet is weak or absent. The crista is absent and the anterior cingulum is weak. The postfossette, formed by the posterior cingulum, is slightly shallower than the median valley. There is a broad entrance to the median valley. A complete metaloph is formed after deep wear.

4.7.2.2. P3 (n = 5, Fig. 6 E–G). The P3 is different from P2 in having both a larger size (Fig. 9A) and a more developed paracone rib and metacone rib. Both parastyle and metastyle are developed on the anterior and posterior ends of the ectoloph, but the latter seems more distinct than the former. The crochet is developed but far from the protoloph. The crista is absent. There are developed anterior and lingual cingulua. The postfossette is formed by the posterior cingulum. The protocone constriction is weak. There is a tiny tuber at the base of metacone. There is a broad entrance to the median valley, which is slightly deeper than the postfossette.

4.7.2.3. P4 (n = 6, Fig. 7 H, I). The basic dental morphology of P4, with a larger width (Fig. 9A), resembles that of P3. The parastyle and metastyle are well developed, and the protocone constriction is weak or even absent. Compared to P3, the paracone rib is similarly distinct, but the metacone rib becomes much weaker or even absent. The crochet is well developed but still far from the protoloph. The crista is basically missing. The entrance to the median valley is much narrower than that of P3 but this can be attributed to differential wear. The median valley is deeper than the postfossette.

4.7.2.4. M1 (n = 6, Fig. 6 J–L). With a nearly square outline and a larger size (Fig. 9 A), the dental morphology of M1 is similar to that of P4. The parastyle is more prominent than in premolars. The distinct paracone rib can extend to the root. The parastyle fold is notable. The ectoloph is clearly inclined to the lingual side, so the crochet is almost approaching the metaloph. The crochet and ectoloph form a sharp angle. There is no trace of a crista. The protocone constriction is slightly more distinct than in P2–P4. The anterior cingulum is developed but has a lower position. The posterior cingulum is developed to form the postfossette, which is equivalent to the median valley in depth. The base of the protoloph is inflated, which can cover two-thirds of the lingual width of the crown. The entrance to the median valley is wide.

4.7.2.5. M2 (n = 6, Fig. 6 M–O). The M2 has a larger size than M1 (Fig. 9 A). The crochet is well developed and close to the metaloph. The crista is usually missing. There is a weak tubercle at the entrance to the median valley on two specimens. The ectoloph is clearly inclined to the lingual side and the metaloph is relatively weak.

4.7.2.6. M3 (n = 8, Fig. 6 P–R). The outline of crown is triangular. The parastyle, paracone rib, and crochet are prominent. The buccal surface of the ectometaloph is flat behind the paracone rib. There is no trace of crista, antecrochet and metacone rib. Two specimens have weak tubercles extending to the median valley on the posterior surface of the protoloph. The anterior cingulum is positioned at the low level but well developed. The posterior cingulum is represented by a series of tiny tubercles at the base of the ectometaloph. The protocone constriction is weak or absent. The base of the protoloph is inflated, which can cover two-thirds of the lingual width of the crown. The entrance to the median valley is wide.

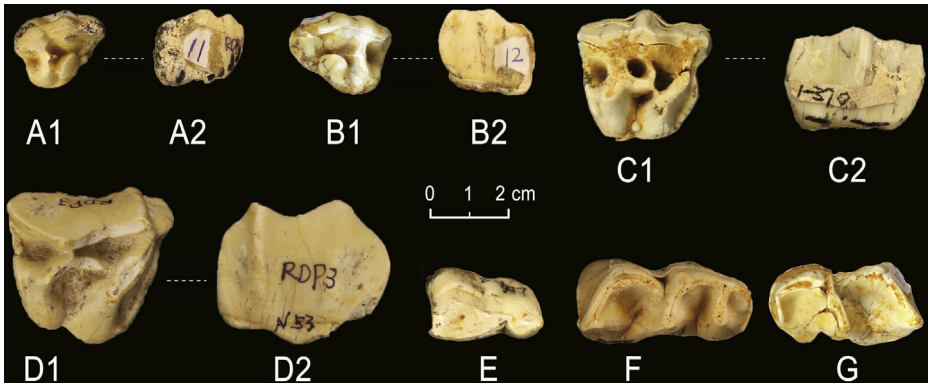

Fig. 5. Upper and lower deciduous dentition of *Rhinoceros fusuiensis* sp. nov. A, right DP1 (V18462.2); B, left DP1 (V18462.4); C, right DP2 (V18462.6); D, right DP3 (V18462.10); E, left dp2 (V18462.62); F, left dp3 (V18462.64); G, right dp4 (V18462.66). A1–D1, E–F, occlusal view; A2–D2, buccal view.

Fig. 6. The upper premolars and molars of *Rhinoceros fusuiensis* sp. nov. A, left P2 (V18462.16); B, right P2 (V18462.18); C, left P2 (V18462.14); D, left P2 (V18462.13); E, left P3 (V18462.25); F, left P3 (V18462.26); G, right P3 (V18462.28); H, right P4 (V18462.34); I, right P4 (V18462.35); J, left M1 (V18462.37); K, left M1 (V18462.38); L, left M1 (V18462.36); M, left M2 (V18462.43); N, left M2 (V18462.42); O, left M2 (V18462.44); P, left M3 (holotype, V18462.47); Q, left M3 (V18462.48); R, right M3 (V18462.54). A1–R1, occlusal view; A2–O2, buccal view; P2–R2, posterior view.

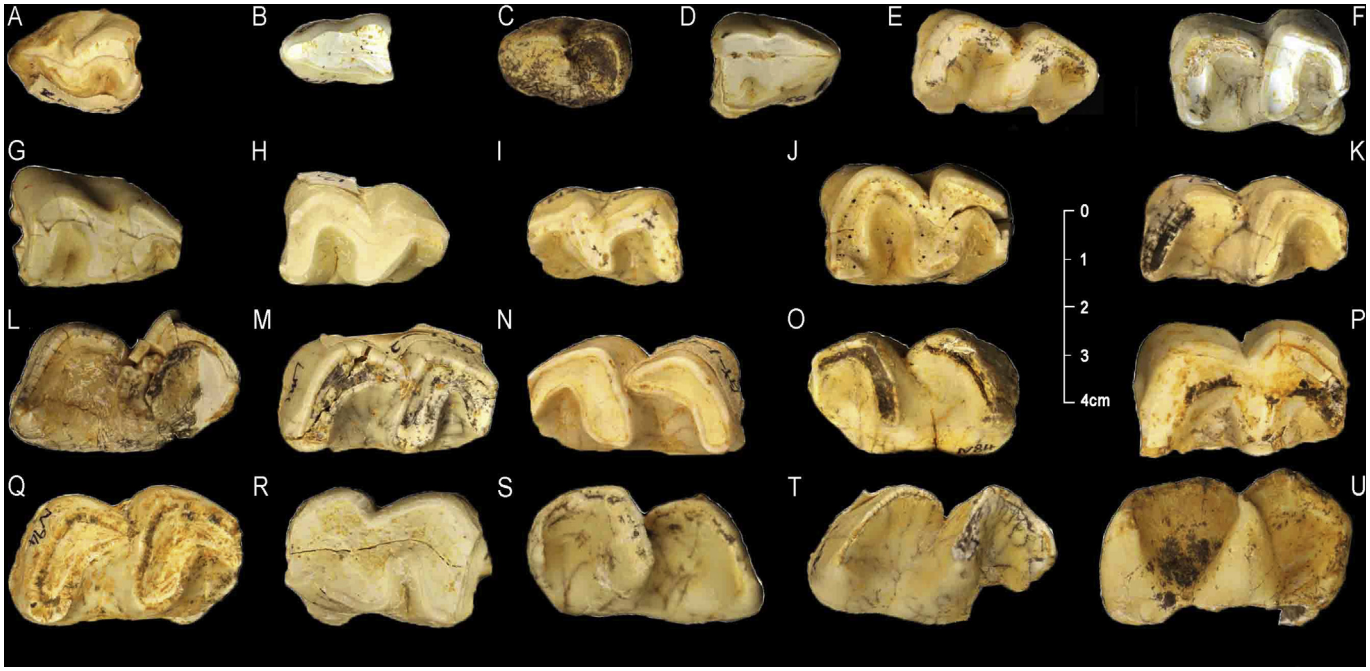

Fig. 7. The lower premolars and molars of *Rhinoceros fusuiensis* sp. nov. A, left p2 (V18462.75); B, left p2 (V18462.80); C, right p2 (V18462.79); D, right p2 (V18462.86); E, left p3 (V18462.89); F, left p3 (V18462.98); G, left p3 (V18462.94); H, left p3 (V18462.96); I, right p3 (V18462.92); J, left p4 (V18462.103); K, left p4 (V18462.105); L, left m1 (V18462.113), M, left m1 (V18462.115); N, right m1 (V18462.120); O, right m1 (V18462.125); P, left m2 (V18462.128); Q, left m2 (V18462.129); R, right m2 (V18462.131); S, right m2 (V18462.132); T, left m3 (V18462.137); U, left m3 (V18462.135). A–U, occlusal view.

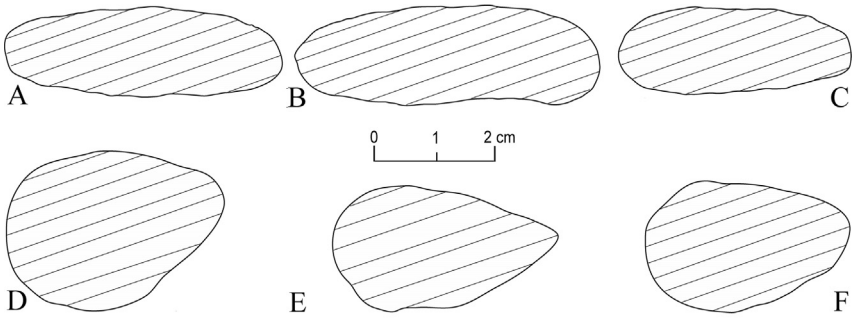

Fig. 8. The transverse sections of upper and lower incisors of *Rhinoceros fusuiensis* sp. nov. Upper incisors: A, V18462. 57; B, V18462. 55; C, V18462. 59. Lower incisors: D, V18462. 142; E, V18462. 159; F, V18462. 160. The sections are drawn at the base of teeth.

4.7.2.7. p2 (n = 18, Fig. 7 A–D). The p2 has a relatively small size (Fig. 9 B). On the specimens with little wear, the paraconid is small, and the protoconid and paraconid are almost fused with each other, leading to an extremely weak metalophid. The paralophid and protolophid are joined together. The hypolophid and entolophid are well developed to form the talonid basin. After heavy wear, the dental morphology becomes simple. The trigonid and talonid are fused to make a triangular outline. The ectoflexid on the buccal side and a trace of talonid basin on the lingual side are observed.

4.7.2.8. p3 (n = 9, Fig. 7 E–I). Compared to p2, p3 has a larger size (Fig. 9 B) and more distinct paralophid. A shallow trigonid basin can be observed on specimens with little wear and a shallow groove on the lingual side is present on the specimens with moderate wear. The protoconid and hypoconid are close to each other or fused after moderate wear. There is an intact talonid basin.

4.7.2.9. p4 (n = 12, Fig. 7 J, K), m1 (n = 13, Fig. 7 L–O), m2(n = 9, Fig. 7 P–S) and m3 (n = 5, Fig. 7 T, U). The dental characters of these teeth are very similar to each other. The lingual main cusps (paraconid, metaconid and entoconid) are higher than the buccal ones (protoconid and hypoconid). The paralophid is distinct. The anterior valley is well separated from the posterior one. The trigonid basin is narrower than the talonid basin. The ectoflexid is evident. The width is gradually increased from p4 to m3, which show wide overlap in the scatter diagram (Fig. 9 B).

4.7.2.10. Upper and lower incisors. The outline of the transverse section of the I1 ($n = 7$) is nearly rectangular in shape (Fig. 8 A–C), and anterior part is rather inflated and the posterior one is flat. On the other hand, the outline of the transverse section of the i2 ($n = 7$) is oval (Fig. 8 D–E).

5. Comparisons

5.1. Comparison with Stephanorhinus and Dicerorhinus

Three genera including *Stephanorhinus*, *Dicerorhinus*, and *Rhinoceros* within the family Rhinocerotidae are known from Southeast Asia (Tong and Moigne, 2000; Tong, 2001; Chen et al., 2012). The *Stephanorhinus* remains differ from Yanliang specimens in having a relatively northern distribution, a large size, the absence of upper and lower incisors, hypsodont upper premolars, a smooth ectoloph, a distinct protocone constriction, and a developed crista (Tong, 2002; Tong and Wu, 2010; Chen et al., 2012). The genus *Dicerorhinus* from Pleistocene localities of Southeast Asia, composed of two species, *Dicerorhinus gwebinensis* and *Dicerorhinus sumatrensis*, is distinguishable from Yanliang specimens by its small size, weak lower incisors with a circular transverse section, a distinct protocone constriction, a moderate crista on M3, and the median valley which is deeper than the postfossette (Pocock, 1945; Hooijer, 1946; Groves and Kurt, 1972; Groves, 1983; Zin-Maung-Maung-Thein et al., 2008).

The Yanliang remains should be assigned to the genus *Rhinoceros* based on the following dental characteristics: a medium size between *Stephanorhinus* and *Dicerorhinus*, presence of upper incisor, a well-developed second lower incisor with an oval transverse section (Fig. 8), the distinct crochet and median valley on upper molars, the same depth of the median valley and postfossette (Pocock, 1945; Groves, 1983; Laurie et al., 1983).

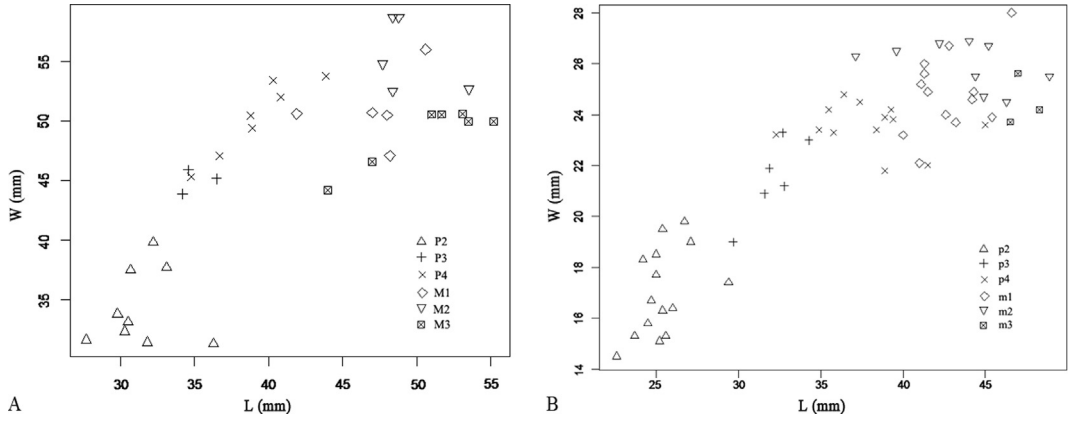

Fig. 9. Scatter diagram of permanent dentition of *Rhinoceros fusuiensis* sp. nov. from Yanliang Cave. A, upper dentition; B, lower dentition; L, mesiodistal length; W, buccolingual width.

5.2. Comparison with *R. sinensis* from the Pleistocene of southern China

Rhinoceros sinensis is the most common Pleistocene species of *Rhinoceros* in southern China. The holotype of *R. sinensis* is an M3 with uncertain provenance (Owen, 1870). Matthew and Granger (1923) listed the specimen, a crushed skull (AMNH 18628) from the Yanjinggou (=Yenchingkou) fauna in Chongqing (formerly Sichuan) as the paratype of *R. sinensis*. After systematic research on the Yanjinggou fauna, Colbert and Hooijer (1953) revised the diagnosis and range of variation *R. sinensis*, and supported its validity.

The understanding of *R. sinensis* is mainly based on the materials from Yanjinggou (Matthew and Granger, 1923; Colbert and Hooijer, 1953). The data present two different assumptions. Firstly, *R. sinensis* remains studied by Matthew and Granger (1923) and Colbert and Hooijer (1953) probably belong to a range of Pleistocene localities in southern China, so the validity of *R. sinensis* is questionable based on unknown spread of geological age (Tong and Moigne, 2000; Tong, 2001; Chen et al., 2012). Secondly, *R. sinensis*, with a relatively large size, is considered to be a synonym of junior *R. unicornis* (Antoine, 2012).

The controversy on the validity of *R. sinensis* mainly resulted from the temporary and ambiguous identification with no detailed description and measurements, and limited comparisons excluding the original materials of *R. sinensis* studied by Owen (1870), Matthew and Granger (1923) and Colbert and Hooijer (1953). The second opinion is untenable because *R. sinensis* differs from *R. unicornis* with a much larger size, a curved ectoloph and the absence of crista on upper molars.

Combined with the descriptions from Matthew and Granger (1923) and Colbert and Hooijer (1953), the diagnosis of *R. sinensis* is revised as follows: The cheek teeth are relatively large and hypsodont because the heights of P3 to M3 are respectively measured as 66–69 mm, 64–74 mm, 79 mm, 75–84 mm, and 64–70 mm (Table 3). The crochet is usually well developed, while the crista is weak or missing. The antecrochet is absent and the postfossette is moderately developed. The P1 is small in size. The parastyle is developed but is weaker than that of *R. sondaicus*. The protocone constriction is distinct on upper molars. The protoloph extends to the median valley, and occupies about two-thirds of the lingual width of the crown. Consequently, *R. sinensis* is considered as the intermediate form between *R. sondaicus* and *R. unicornis* based on the dental morphology (Matthew and Granger, 1923; Colbert, 1942; Colbert and Hooijer, 1953).

Table 3
Height of the upper teeth of different species of *Rhinoceros* (in mm).

	P3	P4	M1	M2	M3
R. sinensis[a]	66–69 (67.5)	64–74 (69)	79	75–84 (79.5)	64–70 (67)
R. sinensis[b]	52.4	52.9		52.8	45–50 (47.5)
R. unicornis[c]	56–68 (62)			72	
R. sondaicus[c]	51		53		
R. fusuiensis sp. nov.	41.2–50				44–45.7 (44.85)

[a] Colbert and Hooijer, 1953.
[b] Zheng, 2004.
[c] Hooijer, 1946.

The *R. sinensis* remains described by Owen (1870) differ from Yanliang specimens in having a larger size, a longer distance between the protocone and hypocone, more developed tubercles on the posterior basal surface of protocone, and a more developed posterior cingulum.

The morphological characters of the Yanjinggou *R. sinensis* remains described by Colbert and Hooijer (1953) are also observed on the Yanliang specimens. Both specimens possess the developed paracone rib and metacone rib on the premolars, the postfossette on the upper teeth, basic absence of antecrochet, and the weak protocone constriction on M3. However, the Yanjinggou *R. sinensis* remains studied by Colbert and Hooijer (1953) are still distinct from the Yanliang specimens by having a large size, more hypsodont cheek teeth, a more developed crista, and a less prominent parastyle.

With a relatively small size and a less hypsodont teeth, the *R. sinensis* remains from the middle Early Pleistocene Longgudong Cave, Jianshi, Hubei (Zheng, 2004) were considered to hold a primitive morphology as compared to *R. sinensis* remains from Yanjinggou. However, the Longgudong remains are still distinguishable from Yanliang specimens with a slightly large size (Tables 2 and 3), the greater W/L ratios of premolars and molars, more distinct protocone constriction on molars, and more occurrence of tuber at the entrance to median valley.

The above comparisons demonstrate that Yanliang remains are different from the typical specimens of *R. sinensis* studied by Owen (1870), Matthew and Granger (1923), and Colbert and Hooijer (1953).

5.3. Comparison with *Rhinoceros* from Southeast Asia

So far, quite a few species of *Rhinoceros* fossils have been reported from Southeast Asia. However, the validity of these species is still controversial (Groves and Kurt, 1972; Laurie et al., 1983; Tougard, 2001; Bacon et al., 2008; Antoine, 2012). For example, the species such as *Rhinoceros kendengindicus* from Java, *Rhinoceros palaeindicus*, *Rhinoceros deccanensis*, *Rhinoceros sinhaleyus*, *R. sivalensis*, and *Rhinoceros kagavena* from Indo-Pakistan are regarded as the junior synonym of *R. unicornis*, however, *R. sivalensis* should not be included in this list. Another species *Rhinoceros philippinensis* from Luzon, Philippines, is also doubtful as a valid taxon because the unequivocal locality and uncertain age (Antoine, 2012). Thus, there are only three valid species of *Rhinoceros* in Southeast Asia besides *R. sinensis* from southern China (e.g., *R. sivalensis*, *R. unicornis* and *R. sondaicus*).

As the earliest species with *Rhinoceros*, *R. sivalensis* from the late Miocene of Siwalik deposits, Indo-Pakistan (Falconer and Cautley, 1847; Falconer, 1867; Colbert, 1935) is different from Yanliang specimens in having a large size (Lydekker, 1881) (Fig. 10), a smooth ectoloph, a weak parastyle, a distinct crochet, a protocone which is more inflated than hypocone, a narrow entrance of the median valley and the same width of protoloph and metaloph.

The *R. unicornis* from the middle Pleistocene to recent of India differs from Yanliang specimens in bearing a larger size (Tables 1 and 2; Fig. 10), more hypsodont cheek teeth (Hooijer, 1946) (Table 3), a smooth ectoloph (Fig. 11), the absence of a parastyle and a parastyle fold, and the existence of a distinct crochet which is often connected with crista to form the medifossette (Colbert, 1942; Pocock, 1945; Laurie et al., 1983).

The *R. sondaicus* from the middle Pleistocene to recent of Java and Sumatra is distinct from Yanliang specimens by having a slightly larger size (Tables 1 and 2; Fig. 10), a more developed crochet, absence of the protocone constriction, a weak metastyle, and a lower crown of upper premolar (Pocock, 1945; Hooijer, 1946; Groves and Leslie, 2011) (Table 3). However, Yanliang specimens are still more similar to the extant species *R. sondaicus* than to other species of the genus in following characteristics of dental morphology: a relatively small size, a well-developed metacone rib on the deciduous dentition, a distinct parastyle fold and curved ectoloph, and the absence of the crista, antecrochet and lingual cingulum.

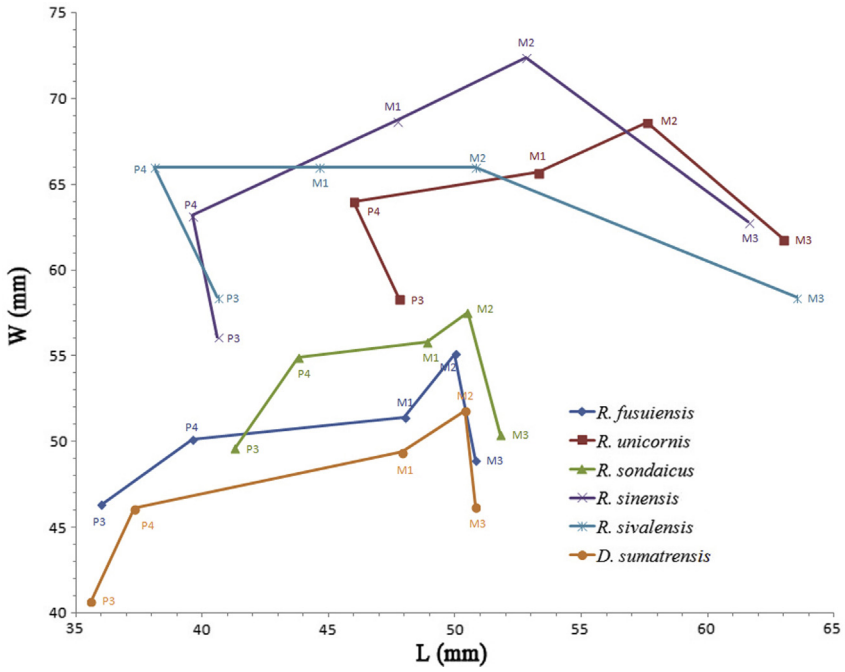

Fig. 10. Line chart showing the average size of the upper cheek teeth of *Rhinoceros fusuiensis* sp. nov. from Yanliang Cave in comparisons with other species of *Rhinoceros* and *Dicerorhinus*. Abbreviation: L = mesiodistal length, W = greatest buccoligual width. *R. unicornis*, *R. sondaicus* and *D. sumatrensis*, Guérin, 1980; *R. sinsensis*, Colbert and Hooijer, 1953; *R. sivalensis*, Lydekker, 1881.

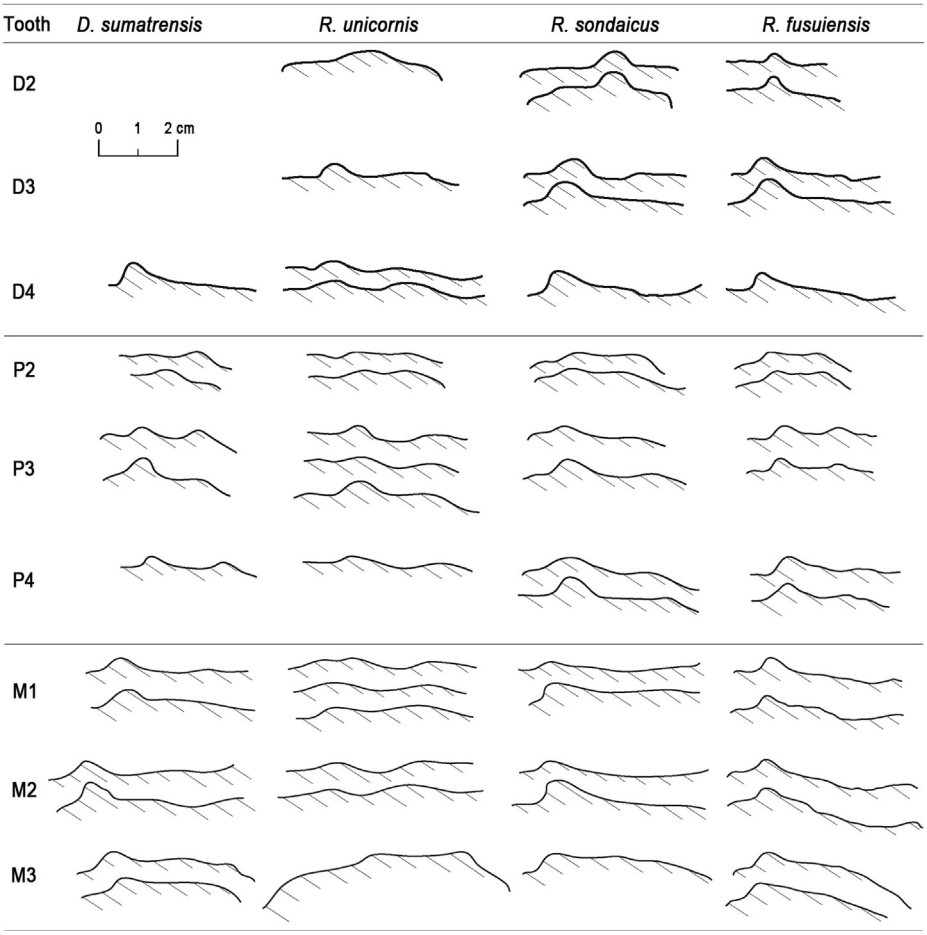

Fig. 11. Comparisons of the ectoloph profile of the upper deciduous teeth, premolars and molar in different species of *Rhinoceros* and *Dicerorhinus*. *R. unicornis*, *R. sondaicus* and *D. sumatrensis*, Guérin, 1980.

As stated above, the *Rhinoceros* remains from Yanliang Cave are identified as a new species, *R. fusuiensis* sp. nov., which is more primitive than *R. sondaicus* in bearing a slightly smaller size, the lesser molarization on P2, the more prominent parastyle on cheek teeth and a more curve ectoloph. The above mentioned differences of dental characteristics also imply *R. fusuiensis* sp. nov. as the potential ancestor of *R. sondaicus*.

6. Discussion

6.1. Other included materials of R. fusuiensis sp. nov.

Based on the dental morphology described above and the related geochronological data, the *Rhinoceros* remain from Longgupo Cave in Chongqing (CV 872.1–4, CV 863–870), Mohui Cave in Guangxi (MH 0063, 0208, 0240, 0479, 0516, 0521, 0533 and 0586; MH, the number of field), and the Irrawaddy sediments at the Pauk area in Myanmar (NMMP-KU-IR 0404, 0408) should be reassigned to *R. fusuiensis* sp. nov. (Fig. 1).

The dental morphology of *R.* cf. *sinensis* from the early Early Pleistocene (1.95 Ma) Longgupo Cave (Huang and Fang, 1991) is similar to that of *R. fusuiensis* sp. nov. from Yanliang Cave in the similar dental size, the distinct paracone rib and metacone rib on the ectoloph of premolars, a well-developed crochet, the distinct anterior cingulum and a broad entrance to the median valley on P4. On M3, both of them share the similar size, a distinct crochet, the absence of metacone rib, a broad entrance to the median valley, and a weak antecrochet.

Wang (2005) and Wang et al. (2005) considered that the *R. sinensis* from the early Early Pleistocene of Mohui Cave (1.80 Ma) with relatively small size and less hypsodont crown, is more primitive than *R. sinensis* from Yanjinggou and is similar to the *Rhinoceros* remain from Longgupo Cave. Both Mohui and Yanliang *Rhinoceros* remains hold the following characteristics: a well-developed crochet which connects crista to form the medifossette, the well-developed anterior and lingual cingula and a distinct mesostyle on upper deciduous molars, and an inflated protocone, a developed crochet which has no contact with protoloph, the absence of metacone rib, and a broad entrance to the median valley on M2.

The *Rhinoceros* remain from the early Pleistocene Irrawaddy sediments at the Pauk area in Myanmar were originally identified as *R. sondaicus* (Zin-Maung-Maung-Thein et al., 2006). After the observation based on the figures, the Myanmar *Rhinoceros* remains are more similar to *R. fusuiensis* sp. nov. than to *R. sondaicus* in bearing the more developed parastyle and better developed metastyle, a weak protocone constriction, a curve buccal surface of the ectoloph, and no trace of lingual cingulum, suggesting that the Myanmar *Rhinoceros* is referred to *R. fusuiensis* sp. nov. Additionally, the geological age of the Myanmar *Rhinoceros* is also corresponding to those of Yanliang, Longgupo and Mohui. The difference of dental size between Yanliang and Myanmar *Rhinoceros* possibly results from their geographical variation.

6.2. Zoogeographical implications of R. fusuiensis sp. nov.

The Fusui area is a part of Indochinese Province which includes southern China, Myanmar, Vietnam, Laos, Cambodia and Thailand (Tougard, 2001). The co-occurrence of fossil *Rhinoceros* and *Dicerorhinus* from the Irrawaddy sediments of Myanmar implies both of them originated in the Asian continent during the Late Miocene to the Early Pleistocene (Zin-Maung-Maung-Thein et al., 2008, 2010). During the late Early Pleistocene, *Rhinoceros* and *Dicerorhinus* began to disperse to Southeast Asia via East Asia (Sino-Malayan Route) rather than via South Asia (Takai et al., 2006; Zin-Maung-Maung-Thein et al., 2010). Here, the new discovery of *R. fusuiensis* sp. nov. from Yanliang Cave, Fusui, Guangxi, as well as *Dicerorhinus sumatrensis* from Liucheng *Gigantopithecus* Cave, Guangxi (Tong and Guérin, 2009) supports this hypothesis. Furthermore, southern China is presumed as an important center of evolution and dispersal for *Rhinoceros* during the Early Pleistocene because of scarcity of this clade from elsewhere of Southeast Asia during that period (Prothero and Schoch, 1989b; Van den Bergh, 2001; Antoine, 2012).

7. Conclusion

Rhinoceros fusuiensis sp. nov. from the early Early Pleistocene Yanliang Cave, Fusui, Guangxi ZAR, southern China differs from other species of *Rhinoceros* on dental morphology. The *Rhinoceros* remains from the Early Pleistocene Longgupo Cave and Mohui Cave in southern China, and Irrawaddy sediments in Myanmar are near-identical with *R. fusuiensis* sp. nov. in dental morphology and therefore they are revised and reassigned into the new species.

Rhinoceros fusuiensis sp. nov., which is regarded as the common element of the early Early Pleistocene *Gigantopithecus-Sinomastodon* fauna in southern China, is best similar to the extant species *R. sondaicus* compared to other species of the genus and is the possible ancestor of *R. sondaicus*.

The phylogenetic relationship between *R. fusuiensis* sp. nov. and *R. sinensis* will require further study and the discovery of additional material of *Rhinoceros*. Given the abundant fossil record, it is possible to infer that southern China represents an important evolutionary and zoogeographic center for *Rhinoceros* during the Early Pleistocene.

Acknowledgements

We greatly appreciate the discussions or field assistance from Haowen Tong, Jiajian Zheng, Wenshi Pan, Dagong Qin, Yingqi Zhang, Min Zhu, Yihong Liu, Zhilu Tang, Qiuyuan Wang and Weimin Zheng. Our thanks go to Zhijie Jack Tseng for his comment and English correction. We are also thankful for the hard work of the guest editor and the anonymous reviewers for their constructive comments to improve the manuscript. This work was supported by the Program of Chinese Academy of Sciences (KZZD-EW-03), National Natural Science Foundation of China (41202017 and 41072013), and the Program of China Geological Survey (1212011220519).

References

Antoine, P.-O., 2012. Pleistocene and Holocene rhinocerotids (Mammalia, Perissodactyla) from the Indochinese Peninsula. Comptes Rendus Palevol 11, 159–168.

Bacon, A.M., Demeter, F., Duringer, P., Helm, C., Bacon, M., The Loang, Vu, Kim Thuy, Nguyen, Antoine, P.,O., Bui, Thi Mai, Mai Huong, Nugyen Thi, Dodo, Y., Chabaux, F., Rihs, S., 2008. The Late Pleistocene Duoi U'Oi Cave in northern Vietnam: paleontological sedimentological, taphonomy and palaeoenvironments. Quaternary Science Reviews 27, 1627–1654.

Colbert, E.H., 1935. Siwalik mammals in the American Museum of Natural History. Bulletin of the American Museum of Natural History 26, 1–401.

Colbert, E.H., 1942. Notes on the lesser one-horned rhinoceros, *Rhinoceros sondaicus*. 2, the position of *Rhinoceros sondaicus* in the phylogeny of the genus *Rhinoceros*. American Museum of Natural History Novitiates 1207, 1–6.

Colbert, E.H., Hooijer, D.A., 1953. Pleistocene mammals from the limestone fissures of Szechwan, China. Bulletin of the American Museum of Natural History 102, 1–134.

Chen, S.K., Huang, W.P., Pei, J., He, C.D., Qin, L., Wei, G.B., Leng, J., 2012. The latest Pleistocene *Stephanorhinus kirchbergensis* from the Three Gorges area and re-evaluation of Pleistocene rhinos in Southern China. Acta Anthropologica Sinica 31, 381–394.

Dong, W., Pan, W.S., Sun, C.K., Xu, Q.Q., Qin, D.G., Wang, Y., 2011. Early Pleistocene ruminants from Sanhe Cave, Chongzuo, Guangxi, South China. Acta Anthropologica Sinica 30, 192–205.

Dong, W., Jin, C.Z., Wang, Y., Xu, Q.Q., Qin, D.G., Sun, C.K., Zhang, L.M., 2013. New materials of Early Pleistocene *Sus* from Sanhe Cave, Chongzuo, Guangxi, South China. Acta Anthropologica Sinica 32, 63–76.
Dong, W., Liu, J.Y., Zhang, L.M., Xu, Q.Q., 2014. Early Pleistocene water buffalo associated with *Gigantopithecus* from Chongzuo in southern China. Quaternary International 354, 86–93.
Falconer, H., Cautley, P.T., 1847. Fauna Antiqua Sivalensis, Atlas. Smith, Elder and Co, London, p. 90.
Falconer, H., 1867. Description of the Plates of the Fauna Antiqua Sivalensis from Notes and Memoranda. Robert Hardwicke, London, p. 136.
Groves, C.P., Kurt, F., 1972. *Dicerorhinus sumatrensis*. Mammalian Species 21, 1–6.
Groves, C.P., 1983. Phylogeny of the living species of Rhinoceros. Zeitschrift fur zoologische Systematik und Evolutionforschung 21, 293–313.
Groves, C.P., Leslie, D.M., 2011. *Rhinoceros sondaicus* (Perissodactyla: Rhinocerotidae). Mammalian Species 43, 190–208.
Guérin, C., 1980. Les rhinoceros (Mammalia, Perissodactyla) du Miocène terminal au Pléistocène supérieur en Europe occidentale. Comparaison avec les espèces actuelles. Documents des Laboratoire de géologie Lyon. Sciences de la Terre 79, 1185.
Han, D.F., 1987. Artiodactyla fossils from Liucheng *Gigantopithecus* Cave in Guangxi. Memoris of Institute of Vertebrate Palaeontology and Palaeoanthropology, Academia Sinica 18, 135–220.
Harrison, T., Jin, C.Z., Zhang, Y.Q., Wang, Y., 2014. Fossil *Pongo* from the Early Pleistocene *Gigantopithecus* faunas of Chongzuo, Guangxi, southern China. Quaternary International 354, 59–67.
Hooijer, D.A., 1946. Prehistoric and fossil rhinoceroses from the Malay Archipelago and India. Zoologische Medeelingen 26, 1–138.
Huang, W.P., Fang, Q.R., 1991. Wushan Hominid Site. Orean Press, Beijing, p. 230.
Jin, C.Z., Qin, D.G., Pan, W.S., Wang, Y., Zhang, Y.Q., Deng, C.L., Zheng, J.J., 2008. Micromammals of the *Gigantopithecus* fauna from Sanhe Cave, Chongzuo, Guangxi. Quaternary Sciences 28, 1129–1137.
Jin, C.Z., Qin, D.G., Pan, W.S., Tang, Z.L., Liu, J.Y., Wang, Y., Deng, C.L., Wang, W., Zhang, Y.Q., Dong, W., Tong, H.W., 2009a. A newly discovered *Gigantopithecus* fauna from Sanhe Cave, Chongzuo, Guangxi, South China. Chinese Science Bulletin 54, 788–797.
Jin, C.Z., Pan, W.S., Zhang, Y.Q., Cai, Y.J., Xu, Q.Q., Tang, Z.L., Wang, W., Wang, Y., Liu, J.Y., Qin, D.G., Edwards, R.L., Cheng, H., 2009b. The *Homo sapiens* Cave hominin site of Mulan Mountain, Jiangzhou District, Chongzuo, Guangxi with emphasis on its age. Chinese Science Bulletin 54, 3848–3856.
Jin, C.Z., Tomida, Y., Wang, Y., Zhang, Y.Q., 2010. First discovery of fossil *Nesolagus* (Leporidae, Lagomorpha) from Southeast Asia. Science China: Earth Sciences 53, 1014–1021.
Jin, C.Z., Wang, Y., Deng, C.L., Harrison, T., Qin, D.G., Pan, W.S., Zhang, Y.Q., Zhu, M., Yan, Y.L., 2014. Chronological sequence of the early Pleistocene *Gigantopithecus* faunas from cave sites in the Chongzuo, Zuojiang River area, South China. Quaternary International 354, 4–14.
Laurie, W.A., Lang, E.M., Groves, C.P., 1983. Rhinoceros unicornis. Mammalian Species 211, 1–6.
Liu, W., Jin, C.Z., Zhang, Y.Q., Cai, Y.J., Xing, S., Wu, X.J., Cheng, H., Edwards, R.L., Pan, W.S., Qin, D.G., An, Z.S., Trinkaus, E., Wu, X.Z., 2010. Human remains from Zhirendong, South China, and modern human emergence in East Asia. Proceedings of the National Academy of Sciences 107, 19201–19206.
Lydekker, R., 1881. Siwalik Rhinocerotidae. Palaeontologia Indica 10, 1–62.
Matthew, W.D., Granger, 1923. New fossil mammals from the Pliocene of Sze-Chuan, China. Bulletin of American Museum of Natural History 8, 63–598.
Mead, J.I., Moscato, D., Jin, C.Z., Wang, Y., this volume. First Pleistocene lizards (Squamata, Reptilia) from the karst caves in Chongzuo, Zuojiang River area of southern China. Quaternary International.
Nowak, R.M., 1999. Walker's Mammals of the World, sixth ed., p. 1936
Owen, P., 1870. On fossil remains of mammals found in China. Journal of the Geological Society 26, 417–436.
Pei, W.Z., 1987. Carnivora, Proboscidea and Rodentia from Liucheng *Gigantopithecus* Cave and other caves in Guangxi. Memoris of Institute of Vertebrate Palaeontology and Palaeoanthropology, Academia Sinica 18, 1–134.
Pocock, R.I., 1945. Some cranial and dental characters of the existing species of Asiatic Rhinoceros. Proceeding Zoological Society London 114, 437–450.
Prothero, D.R., Schoch, R.M., 1989a. Classification of the Perissodactyls. In: Prothero, D.R., Schoch, R.M. (Eds.), The Evolution of Perissodactyls. Oxford University Press, New York, pp. 530–537.
Prothero, D.R., Schoch, R.M., 1989b. Origin and evolution of the Perissodactyla: summary and synthesis. In: Prothero, D.R., Schoch, R.M. (Eds.), The Evolution of Perissodactyla. Oxford University Press, New York, pp. 504–529.
Qiu, Z.X., Wang, B.Y., 2007. Paracerathere Fossils of China. Science Press, Beijing, p. 396.
Takai, M., Saegusa, H., Thaung-Htike, Zin-Maung-Maung-Thein, 2006. Neogene mammalian fauna in Myanmar. Asian Paleoprimatology 4, 143–172.
Tong, H.W., Moigne, A.M., 2000. Quaternary rhinoceros of China. Acta Anthropologica Sinica 19, 257–263.
Tong, H.W., 2001. Rhinocerotids in China-systematics and material analysis. Geobios 34, 585–591.
Tong, H.W., 2002. *Stephanorhinus kirchbergensis*. In: Wu, R.K., Li, X.X. (Eds.), *Homo erectus* from Nanjing. Jiangsu Science and Technology Publishing House, Nangjing, p. 120.
Tong, H.W., Guérin, C., 2009. Early Pleistocene *Dicerorhinus sumatrensis* remains from the Liucheng *Gigantopithecus* Cave, Guangxi, China. Chinese Science Bulletin 42, 525–539.
Tong, H.W., Wu, X.Z., 2010. *Stephanorinus kirchbergensis* (Rhinocerotidae, Mammalia) from the Rhino Cave in Shennongjia, Hubei. Geology 55, 1157–1168.
Tougard, C., 2001. Biogeography and migration routes of large mammal faunas in South-East Asia during the Late Middle Pleistocene: focus on the fossil and extant faunas from Thailand. Palaeogeography, Palaeoclimatology, Palaeoecology 168, 337–358.
Van den Bergh, G.D., De vos, J., Sondaar, P.Y., 2001. The Late Quaternary palaeogeography of mammal evolution in the Indonesian Archipelago. Palaeogeography, Palaeoclimatology, Palaeoecology 171, 385–408.
Wang, W., Potts, R., Hou, Y.M., Chen, Y.F., Wu, H.Y., Yuan, B.Y., Huang, W.W., 2005. Early Pleistocene hominid teeth recovered in Mohui cave in Bubing Basin, Guangxi, South China. Chinese Science Bulletin 50, 2777–2782.
Wang, W., 2005. Early Pleistocene Hominoid Fossil Assemblage from Mohui Cave, Tiandong County, Guangxi, South China and its Significance of Early Human Evolution (PhD thesis). University of Geosciences, Department of Geology, China, p. 150.
Wang, W., Potts, R., Yuan, B.Y., Huang, W.W., Cheng, H., Edwards, R.L., Ditchfield, P., 2007. Sequence of mammalian fossils, including hominoid teeth, from the Bubing Basin caves, South China. Journal of Human Evolution 52, 370–379.
Wang, W., 2009. New discoveries of *Gigantopithecus blacki* teeth from Chuifeng Cave in the Bubing Basin, Guangxi, south China. Journal of Human Evolution 57, 229–240.
Wang, Y., Qin, D.G., Jin, C.Z., Pan, W.S., Zhang, Y.Q., Zheng, J.J., 2009. Murid Rodents of the new discovered fauna from the Sanhe Cave, Chongzuo, Guangxi, South China. Acta Anthropologica Sinica 28, 73–87.
Wang, Y., Jin, C.Z., Zhang, Y.Q., Qin, D.G., 2010. Murid rodents from the *Homo sapiens* Cave of Mulan Mountain, Chongzuo, Guangxi, South China. Acta Anthropologica Sinica 29, 303–316.
Wang, Y., Jin, C.Z., Mead, J.I., 2014. New remains of *Sinomastodon yangziensis* (Proboscidea, Gomphotheriidae) from Sanhe karst cave, with discussion on the evolution of Pleistocene *Sinomastodon* in South China. Quaternary International 339–340, 90–96. http://dx.doi.org/10.1016/j.quaint.2013.03.006.
Wu, W.T., 1983. On the two rhinoceros subfossils from Hemudu Neolithic Site. Vertebrata PalAsiatica 20, 160–165.
Zhang, Y.Q., Jin, C.Z., Takai, M., 2010. A partial skeleton of *Macaca* (Mammalia, Primtes) from the Early Pleistocene Queque Cave site, Chongzuo, Guangxi, South China. Vertebrata PalAsiatica 48, 275–280.
Zhang, Y.Q., Jin, C.Z., Cai, Y.J., Kono, R., Wang, W., Wang, Y., Zhu, M., Yan, Y.L., 2014. New 400–320 ka *Gigantopithecus blacki* remains from Hejiang Cave, Chongzuo City, Guangxi, South China. Quaternary International 354, 35–45. http://dx.doi.org/10.1016/j.quaint.2013.12.008.
Zhao, L.X., Jin, C.Z., Qin, D.G., Pan, W.S., 2008. Description of new fossil teeth of *Gigantopithecus blacki* from Sanhe Cave, Chongzuo, Guangxi Southern China with comments on evolutionary trends in *Gigantopithecus* dental size. Quaternary Sciences 28, 1139–1144.
Zheng, S.H., 2004. Jianshi Hominid Site. Science Press, Beijing, p. 412.
Zin-Maung-Maung-Thein, Thaung-Htike, Tsubamoto, T., Takai, M., Egi, N., Maung-Maung, 2006. Early Pleistocene Javan rhinoceros from the Irrawaddy Formation, Myanmar. Asian Paleoprimatology 4, 197–204.
Zin-Maung-Maung-Thein, Takai, M., Tsubamoto, T., Thaung-Htike, Egi, N., Maung-Maung, 2008. A new species of *Dicerorhinus* (Rhinocerotidae) from the Plio-Pleistocene of Myanmar. Paleontology 51, 1419–1433.
Zin-Maung-Maung-Thein, Takai, M., Takehisa, T., Egi, N., Thaung-Htike, Nishimura, T., Maung-Maung, Zaw-Win, 2010. A review of fossil rhinoceros from the Neogene of Myanmar with description of new specimens from the Irrawaddy sediments. Journal of Asian Earth Sciences 37, 154–165.